18th Brazilian Congress of Thermal Sciences and Engineering
November 16-20, 2020 (Online)

ENC-2020-0012
CONVECTIVE HEAT TRANSFER IN A CHANNEL WITH PROTRUDING INTERNAL HEAT GENERATING BODIES

Paulo Mohallem Guimarães
Rogério Fernandes Brito
Leonardo Rodrigues Martins Pereira
Arthur Gomes Paiva
Universidade Federal de Itajubá – Campus Itabira
pauloguimaraes@unifei.edu.br
rogbrito@unifei.edu.br
leormpereira@gmail.com
arthur.gp1532@gmail.com

Renato José Pinto
Centro Universitário da FEI
rjpinto@fei.edu.br

Genésio José Menon
Universidade Federal de Itajubá – Campus Itajubá
genesio@unifei.edu.br

Abstract. *This work presents a numerical laminar study of conjugate heat transfer of air flow in a rectangular channel with conductive and internal energy generating sources placed on the channel bottom wall. The finite element method is applied to approximate solutions to the conservation equations in terms of stream function, temperature, and vorticity. This work aims to analyze the temperature and velocity fields, and the heat transfer in terms of Nusselt number. Some geometric and physical parameters are considered as follows: Grashof number from 0 to 10^6, Prandtl number equal to 0.7, Reynolds number from 10 to 1000 and diffusivities from 3 to 100, three source heights and channel inclinations of 0^0, 45^0 and 90^0.As it is expected, some recirculations and thermal wake appeared due to the presence of the heat generating bodies. The effect of the inclination angle study showed that the horizontal channel position presented a lower average Nusselt number for the first and third bodies. However, for body 3, this difference was much more significant. There was no significant difference in Nu between 45^o and 90^0 for body 3.*

Keywords: *mixed convection, internal heat generation, protruding heat sources, finite element method*

1. INTRODUCTION

The heat transfer study inside channels and cavities have brought about works in the scientific academy due to their applications such as cooling of electronic component that must work within allowable temperature limits in order to guarantee more appropriate functioning. For instance, electronic component miniaturization may lead to higher heat transfer rates. In literature, one can find many studies that were carried out experimentally and numerically concerning a better understanding of heat and fluid flow in order to enhance removal of heat generated in operating components.

It is worth mentioning that food industry, heat exchangers, nuclear reactors, chemical process equipment, heating systems, environmental control systems, among others, are applications where heat transfer phenomenon always demands better understanding in order to improve their thermal performance.

Mikhailenko et al. (2018) studied the convective-radiative heat transfer in passive cooling systems for electronic devices inside rotating cavities with local heat-generating elements. Such analysis provided optimal parameters in order to decrease the working temperature of the heated unit. The cavities have horizontal and vertical walls are adiabatic and uniformly cold, respectively. A mathematical model was developed using the stream function, vorticity and temperature variables. It was approximated by the finite difference method. It was shown the influence of surface emissivity, Taylor number, and Ostrogradsky number on streamlines, isotherms, average Nusselt number, fluid flow rate and average temperature inside the heater. It has been found that in the case of heat generating and heat-conducting element the periodicity in fluid flow intensity and heat transfer rates could be observed after a lot of complete revolutions. The

increase in surface emissivity essentially reduced the average temperature inside the heated element, while an intensive rotation also provided lower temperature in the heated body.

Xu et al. (2016) carried out an experimental work to control temperature distribution in high-power electronic devices with multiple heating elements that require temperature uniformity within a range for an optimal performance. The apparatus consisted of a computer-controlled pump, a multi-channel heat sink for multi-zone cooling, and sensors to measure temperature and pressure drop. The structure design targeted a minimum pumping power with a uniform temperature distribution as well as a low peak temperature, especially for a non-uniform initial heat flux or temperature condition.

Kuznetsov and Maksimov (2016) conducted an experimental investigation of mixed convection of a gas in a rectangular enclosure with a local heat source. Heat was removed through outer boundaries. The experiments have shown that a system providing a thermal regime in a closed space with a mixed convection can be self-regulated. It was established that an intensification of the heat generation in such a space leads to the transformation of the vortex structures that form over the energy source and carry heat to the periphery of the space. The larger the power of the energy source, the higher the velocity of the gas flow and the larger the dimensionless heat-transfer coefficient (the Nusselt number) at the entire air–fencing wall interfaces. The dependence between these two characteristics is nonlinear. It should be noted that all the investigations were performed for the regime of purely convective heat exchange without regard for the possible radiation heat transfer. In the case of highly intense heat generation, the temperature of the gas increases. As a result, the contribution of the radiative heat flow to the total heat flow can increase, which plays a decisive role in some regimes. This hypothesis is supported by the fact that the heat transfer in gas–particles–imitators system intensifies in the case of illumination of this system by a powerful light source.

Muthtamilselvan et al. (2014) investigated the effect of space and temperature dependent heat generation/absorption on an unsteady laminar boundary layer flow of viscous, incompressible, radiating and electrically conducting fluid over a vertical stretching permeable surface. Magnetic field and buoyancy forces were considered. By applying similarity analysis, the governing partial differential equations were transformed into a set of non-linear coupled ordinary differential equations that were solved by Runge-Kutta-Fehlberg method along with shooting technique. One of the main conclusions was that the value of the local Nusselt number decreases with increasing buoyancy parameter and Prandtl number. Nevertheless, the Nusselt number increases by increasing the following: magnetic parameter, variable thermal conductivity parameter, heat generation parameter and thermal radiation parameter.

Guimarães and Menon (2011) studied the effect of mixed convection of air in a rectangular channel having flushed heat sources. Three distinct situations are carried out: i) one heat source, where Reynolds and Grashof numbers, and inclination angle are varied. For this case, it was observed that the inclination angle has a more significant effect on Nusselt number lower Reynolds numbers. There was no expressive difference in Nusselt number for angles of 45º and 90º. The second situation considers 2 heat sources in horizontal rectangular channels where the distance between them is varied as well as Reynolds number ($1 \leq Re \leq 1000$), and Grashof number (10^3, 10^4 e 10^5). It is observed heat wakes strongly interfere on the second body in terms of weakening heat transfer as the distance between the sources is decreased. The third situation with three heat sources equally spaced is studied being that the heat transfer is strongly influenced by the channel inclination for low Reynolds numbers.

Bautista and Méndez (2006) conducted an analytical and numerical work to study the heat transfer in a rectangular-channel in order to cool a discrete heat source within it. A constant and uniform volumetric heat generation is provided by a heated strip embedded in a substrate. The governing equations for the refrigerant fluid and solid domains are reduced to an integral-differential equation. It was shown that the heat transfer process in this conjugate problem was controlled by a parameter that determines the regime between the refrigerant and the discrete heat source.

This work aims to study numerically the mixed convection inside a channel with three discrete conductive heat sources with internal heat generation. The finite element method is used to approximate solutions considering steady and non-steady laminar and two-dimensional regime. It brings analysis on distributions of dimensionless variables such as streamline (ψ), vorticity (ω) and temperature (θ). In addition, local and average Nusselt numbers are calculated in terms of geometrical and thermal parameters to give the heat transfer gradient on the interface surface between the solid and fluid domains. In addition to this, maximal ad average temperatures are obtained on the same surfaces where Nusselt number is calculated. The geometrical parameters that are investigated are the body heights (H_B = 0.075, 0.1, and 0.15) and the channel inclinations 0º, 45º, and 90º .Some physical parameters are investigated: Reynolds number from 10 to 1000, the Grashof number from 1 to 10^6, Prandtl number equals 0.7 (air), diffusivities ratio (solid/fluid) from 10 to 100.

2. PROBLEM DESCRIPTION AND MATHEMATICAL MODELING

The problem consists of: i) a fluid domain (Ω_f), and ii) a solid domain (Ω_s), where mixed convection and conduction take place, respectively.

Figure 1 depicts the geometry of a channel with length A and height 1. Air enters S_1 with constant and uniform profiles of velocity u_0, pressure p_0, and low temperature T_c. S_2 and S_3 are adiabatic, except on the locations where three heat-generating bodies are placed on S_2. These protruding bodies have width B and height H_B. Air exits the channel on

S_4. S_5 is the interface surface between the solid and fluid domains. Not only the body height (H_B), but also, the channel inclination (α) is varied as mentioned before. The channel is featured by: the dimensionless channel length (A = 6.5); the body width (B = 0.5); position of the first, second and third bodies are, respectively, X_1 = 0.5; X_2 = 1.0, X_3 = 1.0; and X_4 = 2.5.

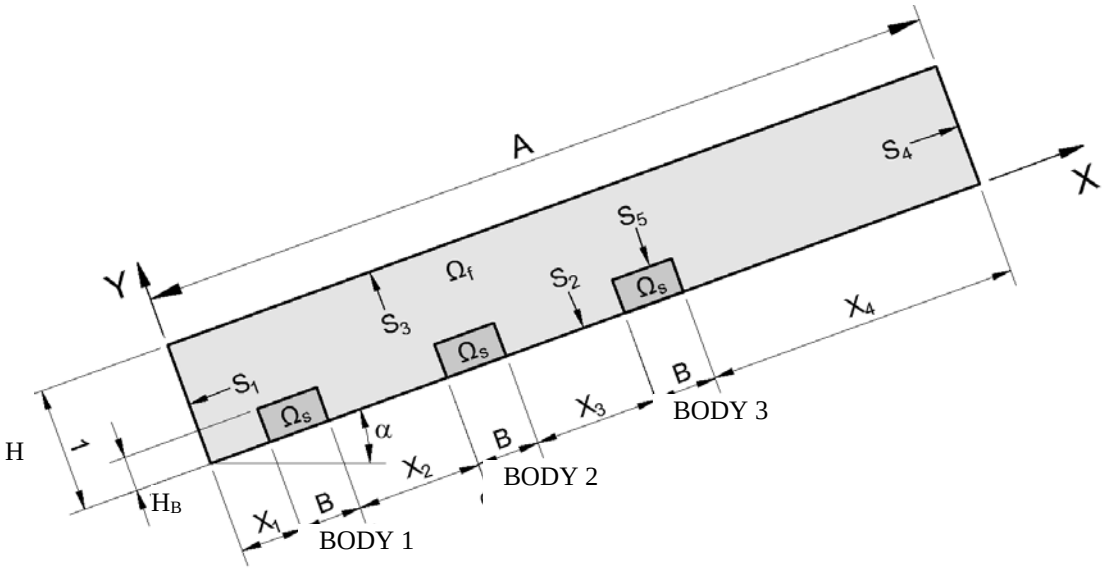

Figure 1. Geometry, surfaces, and domains.

The problem is carried out under the following conditions:

a) For the fluid domain (Ω_f)

- transient regime;
- two-dimensional and laminar flow;
- incompressible flow;
- viscous dissipation function is neglected;
- constant fluid physical properties ($\rho_f, \mu_f, \nu_f, c_{pf}, \alpha_f, k_f$), where μ_f is the dynamics viscosity, ν_f is the kinematics viscosity, c_{pf} is the specific heat at constant pressure, α_f is the thermal diffusivity, and k_f is the thermal conductivity, and ρ_f is the constant density, except the density in the buoyancy terms where the Boussinesq approximation is applied.
- no internal heat generation in the fluid.

b) For the solid domain (Ω_s - u and v are zero)

- transient regime;
- constant physical solid properties (ρ_s , c_{ps} , k_s), where ρ_s is the density ; c_{ps} is the specific heat at constant pressure, and k_s is the thermal conductivity;
- there is internal heat generation.

In order to reduce the number of parameters and to generalize the numerical approximation, the conservation equations are rewritten in the dimensionless form by using the following dimensionless parameters:

$$\tau = \frac{u_o\, t}{H}, \quad X = \frac{x}{H}, \quad Y = \frac{y}{H}, \quad U = \frac{u}{u_o}, \quad V = \frac{v}{u_o}, \quad P = \frac{p}{\rho_f\, u_0^2}, \quad \theta = \frac{T - T_c}{\Delta T}; \; B = b/H \tag{1}$$

where the dimensional quantities are: time (*t*); fluid velocities in *x* (*u*) and y (*v*) directions, body width (b)temperature (*T*), pressure (p), gravity acceleration (g), volumetric expansion coefficient (β), the reference temperature (T_c) and the channel inclination angle (α), and the dimensionless quantities are: time (τ), velocities *U* and *V* in X and Y directions, respectively, pressure (*P)*, temperature(θ), body width (B) and ΔT is given by:

$$\Delta T = \frac{q''' H^2}{k_f} \tag{2}$$

where q''' is the volumetric energy generation rate.

The dimensionless conservation equations are, therefore, given by the following:

a) For the fluid domain (Ω_f):

Dimensionless mass conservation equation:

$$\frac{\partial U}{\partial X} + \frac{\partial V}{\partial Y} = 0 \tag{3}$$

Dimensionless momentum conservation equation:

$$\frac{\partial U}{\partial \tau} + U\frac{\partial U}{\partial X} + V\frac{\partial U}{\partial Y} = -\frac{\partial P}{\partial X} + \frac{1}{Re}\left(\frac{\partial^2 U}{\partial X^2} + \frac{\partial^2 U}{\partial Y^2}\right) + Ri\,\theta\, sen\alpha \tag{4}$$

$$\frac{\partial V}{\partial \tau} + U\frac{\partial V}{\partial X} + V\frac{\partial V}{\partial Y} = -\frac{\partial P}{\partial Y} + \frac{1}{Re}\left(\frac{\partial^2 V}{\partial X^2} + \frac{\partial^2 V}{\partial Y^2}\right) + Ri\,\theta\cos\alpha \tag{5}$$

Dimensionless energy conservation equation:

$$\frac{\partial \theta}{\partial \tau} + U\frac{\partial \theta}{\partial X} + V\frac{\partial \theta}{\partial Y} = \frac{1}{Pr\,Re}\left(\frac{\partial^2 \theta}{\partial X^2} + \frac{\partial^2 \theta}{\partial Y^2}\right) \tag{6}$$

where Re is the Reynolds number, Ri is the Richardson number, Pr is the Prandtl number, and Gr is the Grashof number given by:

$$Re = \frac{u_o H}{\nu_f}, \quad Ri = \frac{Gr}{Re^2}, \quad Gr = \frac{g\,\beta\,\Delta T\,H^3}{\nu_f^2}, Pr = \frac{\nu_f}{\alpha_f} = \frac{\mu_f\,c_{pf}}{k_f} = \frac{\rho_f\,\nu_f\,c_{pf}}{k_f} \tag{7}$$

b) For the fluid domain (Ω_s):

Dimensionless energy conservation equation:

$$\frac{\partial \theta}{\partial \tau} = \frac{D}{Pr\,Re}\left(\frac{\partial^2 \theta}{\partial X^2} + \frac{\partial^2 \theta}{\partial Y^2}\right) + S \tag{9}$$

$$D = \frac{\alpha_s}{\alpha_f}, \quad S = \frac{q'''H}{\rho_S\,c_{ps}\,u_o\,\Delta T} = \frac{D}{Pr\,Re} \tag{10}$$

$$\alpha_f = \frac{k_f}{\rho_f\,c_{pf}}; \alpha_S = \frac{k_s}{\rho_S\,c_{pS}} \tag{11}$$

where D is diffusivity ratio of solid and fluid, S is the dimensionless energy generation in the solid domain and α_s is solid diffusivity and α_f is the fluid diffusivity

The stream function ψ and vorticity ω are defined as:

$$U = \frac{\partial \psi}{\partial Y} \text{ and } V = -\frac{\partial \psi}{\partial X} \tag{12}$$

$$\omega = \frac{\partial V}{\partial X} - \frac{\partial U}{\partial Y} \tag{13}$$

After substituting these definitions into the dimensionless conservation equations, one can write the conservation equations in terms of stream function and vorticity as follows:

$$\frac{\partial^2 \psi}{\partial X^2} + \frac{\partial^2 \psi}{\partial Y^2} + \omega = 0 \tag{14}$$

$$\frac{1}{Re}\left(\frac{\partial^2 \omega}{\partial X^2} + \frac{\partial^2 \omega}{\partial Y^2}\right) + \left(\frac{\partial \psi}{\partial X}\frac{\partial \omega}{\partial Y} - \frac{\partial \psi}{\partial Y}\frac{\partial \omega}{\partial X}\right) + Ri\frac{\partial \theta}{\partial X}\cos\alpha - Ri\frac{\partial \theta}{\partial Y}sen\alpha = \frac{\partial \omega}{\partial \tau} \tag{15}$$

$$\frac{1}{Pr\,Re}\left(\frac{\partial^2 \theta}{\partial X^2} + \frac{\partial^2 \theta}{\partial Y^2}\right) + \left(\frac{\partial \psi}{\partial X}\frac{\partial \theta}{\partial Y} - \frac{\partial \psi}{\partial Y}\frac{\partial \theta}{\partial X}\right) = \frac{\partial \theta}{\partial \tau} \tag{16}$$

The energy equation is the same for the solid domain.

The initial and boundary conditions are given by:

i) initial conditions ($\tau = 0$):

$$\theta = 0\,, \psi = \omega = 0 \text{ (on } \Omega \text{)} \tag{17}$$

ii) boundary conditions ($\tau > 0$):

$$\theta = 0\,,\ \psi = Y\,,\ \omega = 0 \text{ (on } S_1\text{)} \tag{18a}$$

$$\frac{\partial \theta}{\partial n} = 0\,, \psi = 0\,, \omega = \omega_M \text{ (on } S_2\text{)} \tag{18b}$$

$$\frac{\partial \theta}{\partial n} = 0\,,\ \psi = 1\,,\ \omega = \omega_M \text{ (on } S_3\text{)}, \tag{18c}$$

$$\frac{\partial \theta}{\partial n} = \frac{\partial \psi}{\partial n} = \frac{\partial \omega}{\partial n} = 0 \text{ (on S}_4\text{)}, \tag{18d}$$

The average Nusselt numbers is given by:

$$Nu = \frac{1}{L_c}\int_0^{L_c} Nu_L\big|_S \, dS = \frac{1}{L_c}\int_0^{L_c} \frac{1}{\theta}\frac{\partial \theta}{\partial \bar{n}}\bigg|_S \, dS\,, \tag{19}$$

where L_c is the dimensionless length of the line that refers to the interface surface between solid and fluid.

3. VALIDATION, MESH INDEPENDENCY AND TIME STEP STUDY

This section is extensively found in the work of Pinto (2016). Only main aspects are shown here due to a matter of space.

The finite element method is used to approximate solutions to the problem. Two validations were carried out.The first one is a two dimensional laminar and incompressible flow in a backward-step channel, and the second one is a

rectangular channel with two-dimensional, laminar, and incompressible flow heated from below. The results were contrasted with experimental and numerical ones, resulting in excellent agreement.

Also, a thorough mesh independency study is performed taking into account different bodies heights, where the average Nusselt numbers, maximum and average temperatures are investigated. The number of elements varied from about 4000 to 14000. The maximum deviation noted was 1.47% from the previous mesh with about 13000 elements. This study is not found here.

Many time steps were considered. The dimensionless time-step $\Delta\tau = 10^{-3}$ was chosen to run the remaining simulations in this work.

4. RESULTS

Figure 2 presents the average Nusselt number, Nu_B, on bodies 1 (a) and 3(b), versus Grashof number for H_B = 0.075, 0.1, and 0.15, Pr =0.7, Re = 100, D = 5 and α = 0º. All bodies are placed following the dimensionless geometrical parameters: L = 6.5; B = 0.5; X_1 = 0.5; X_2 = 1.0, X_3 = 1.0; and X_4 = 2.5, and H = 1. Nu_B increases for all heights as Gr increases. However, if one fixes Gr to one value up to 3.10^5, Nu_B in body 1 is the highest for H_B = 0.150 and the lowest for H_B = 0.075. This behavior comes to be the opposite for Gr ≥ 8.10^5 and the three bodies present a more significant difference in Nusselt number. This happens due to for high Gr, buoyancy forces are predominant and even more predominant for bigger bodies since the energy generation is a volumetric effect. Also, bodies for H_B = 0.15 may stimulate recirculation that can impair heat exchange. Case (b) does not show this behavior and the Nusselt numbers for all three heights tend to be the same. It is worth mentioning that body 3 faces a thermal wake that body 1 does not, leading to lower Nusselt numbers.

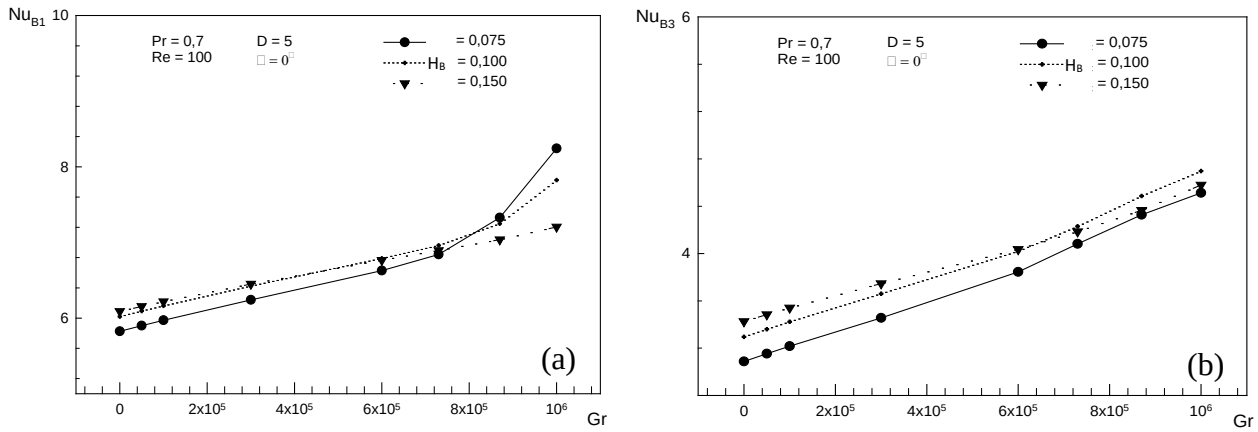

Figure 2. Average Nusselt number on bodies 1(a) and 3(b), Nu_{B3}, versus Grashof number, Gr.

Figure 3 pictures the average Nusselt number, Nu_B, on bodies 1, 2, and 3 versus Re for Pr = 0.7, H_B = 0.075, Gr = 10^5, D = 5, and α = 0º. As it is expected, Nu_B on body 1 is higher due to it is the first hot body to meet to cold fluid which is entering the channel. One can observe that, interestingly, Nu_{B2} and Nu_{B3} are quite the same. One may expect to have lower Nu on downstream bodies in an asset like this, but they are almost equal. In fact, it depends on the distance between bodies, Re, and Gr, which interfere in this thermal wake that leads to heating of subsequent hot bodies.

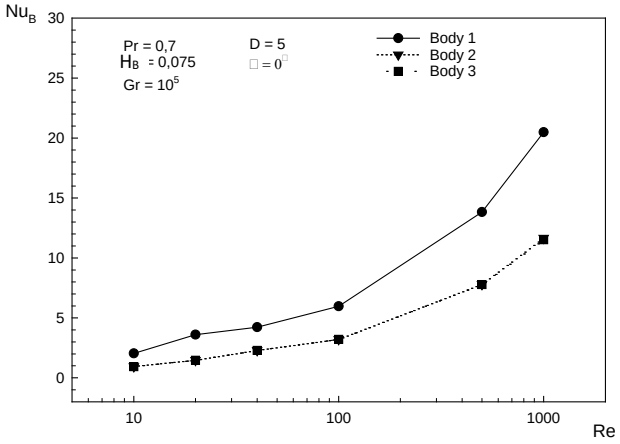

Figure 3. Average Nusselt number, Nu, versus Re for Pr = 0.7, H_B = 0.075, Gr = 10^5, D = 5, and α = 0º.

Figure 4 denotes the effect of diffusivity, D = 3, 5, 10, 50, and 100 on Nu_B for bodies 1 (a) and 3(b), respectively, and Gr = 10^5, H_B = 0.075, Re = 100, and α =0º. An increase in D means an increase of the solid diffusivity, and hence, the temperature field and thermal gradients inside the solid body are reduced and tends to be more uniform due to heat transfer rate resistance. This effect intensifies the heat exchange between the solid and fluid. This is valid for every Grashof number range used in this work.

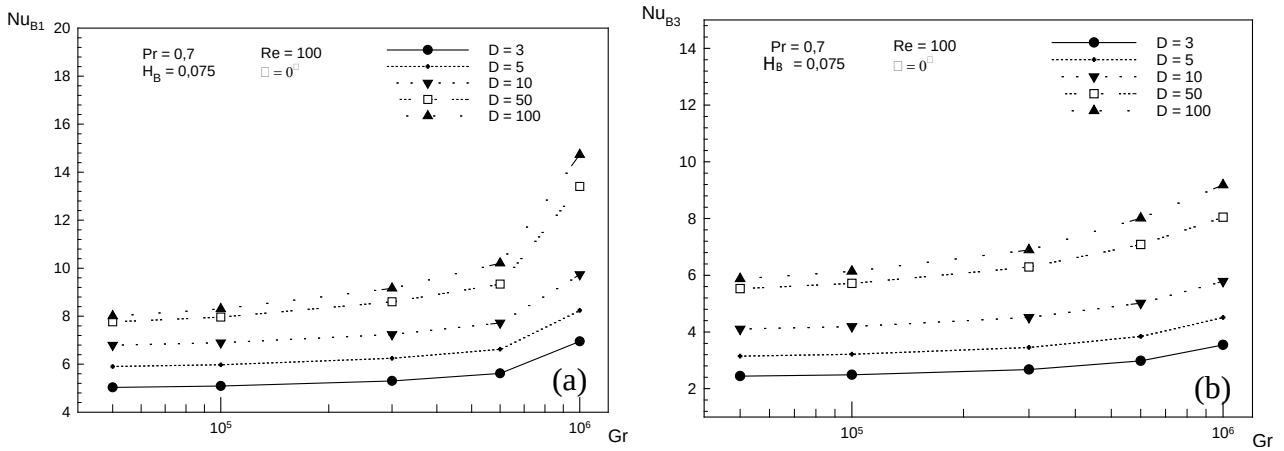

Figure 4. Average Nusselt number on body 1 (a) and 3(b), Nu_{B1}, versus Gr for D = 3, 5, 10, 50, and 100, α = 0.

The effect of the inclination angle may be observed in Figs. 5 versus Gr for bodies 1(a) and 3(b), respectively, for α = 0º, 45º and 90º, Pr = 0.7, Re = 100, H_B = 0.150 and D = 5. In Fig.5(a), the horizontal channel position presents a lower Nu_B for every Gr and both bodies. However, for body 3, this difference is much more significant. In Fig. 5(b), there is no significant difference in Nu between 45º and 90^0.

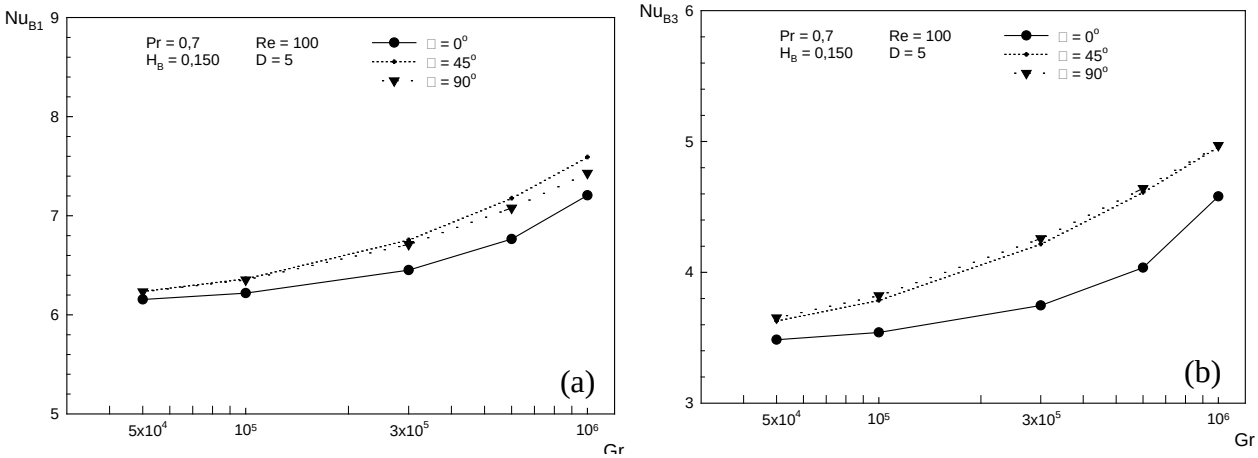

Figure 5. Average Nusselt number on body 1(a) and 3(b), Nu_{B1}, versus Gr for D = 5, α = 0º, 45º, and 90º.

Figure 6 depicts the dimensionless temperature (θ) distribution on bodies 1, 2 and 3 for H_B = 0,150, Re = 500, Pr = 0.7, Gr = 10^5, D = 5, and α =0º. The maximum temperature found is 0.082 on body 3, as it was previously mentioned.

Figures 7 shows the isotherms and stream functions for Re = 100, 300, 500, 1000, Pr = 0.7, D = 5, α = 0º, H_B = 0.15, τ = 20, and Gr = 10^6. For the cases studied, there was no quasi-periodic behavior in time. The least favorable case is for Re = 100. In this case, there is a strong reversal flow in the upper part of the channel. For higher Re (Re>100), this situation is softened due to stronger forced velocities that impairs recirculation and formation of convective plumes in the regions just above the bodies, and thus, facilitating the cooling of the bodies and hence presenting lower temperatures.

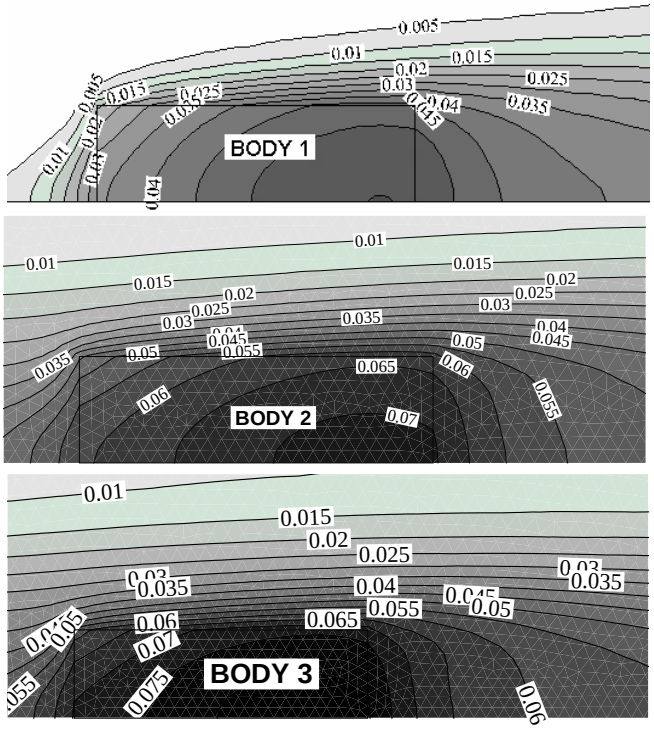

Figure 6. Dimensionless temp. (θ) on bodies 1, 2, and 3 for Re = 500, Pr = 0.7, Gr = 10^5, D = 5, α =0º, and H_B = 0.150.

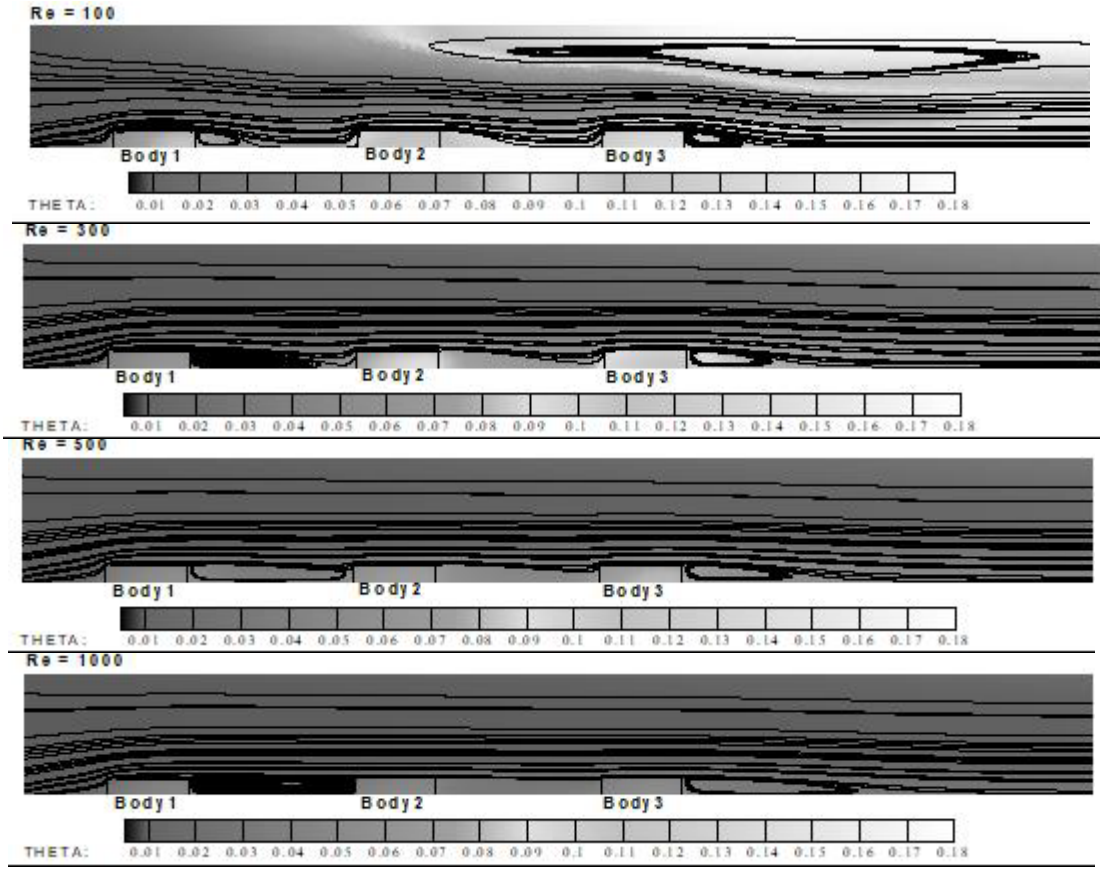

Figure 7 – Dimensionless temperature field θ, stream function ψ , for H_B = 0.150, Pr = 0,7; D = 5, α = 0, Gr = 10^6.

Figure 8 denotes the behavior of flow and of temperature for different body heights for Re = 100, D = 5, α = 0º and Gr = 10^6. A recirculation appears in the upper part of the channel and it tends to weaken, as there are higher bodies. Higher bodies promote smaller channel section. Since the mass flow has to be conserved, one expects higher velocities for higher H_B. Interestingly, Fig. 2b shows that the case with H_B = 0.10 in Fig. 8 presents a slightly higher heat transfer.

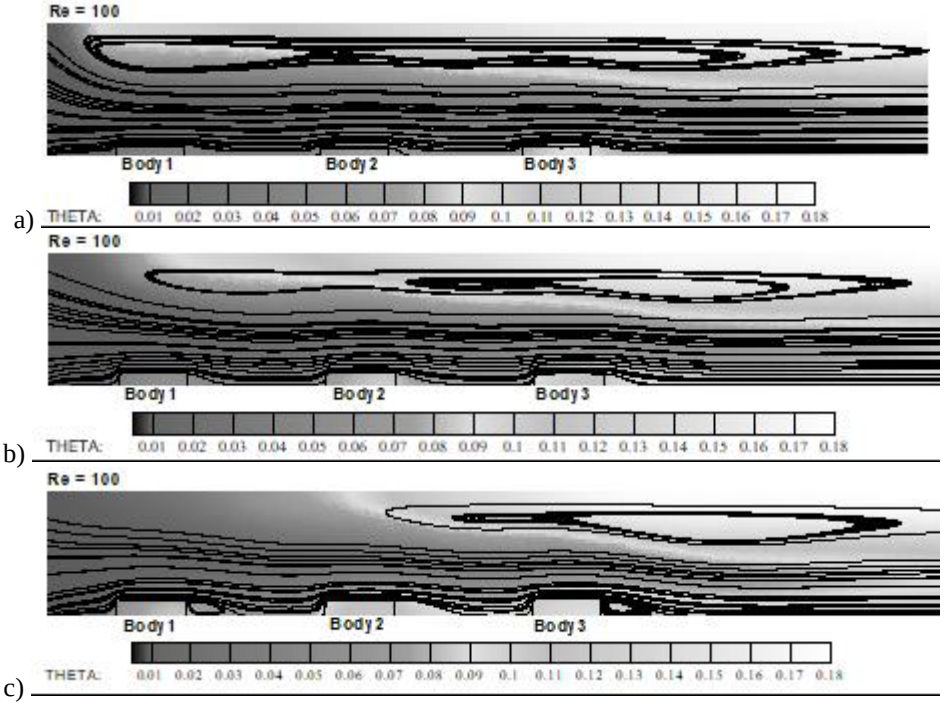

Figure 8. Temperature and streamlines for different body heights for Re = 100, D = 5, α = 0º and Gr = 10^6.

5. CONCLUSION

This work numerically studied a conjugate heat transfer of airflow in a rectangular channel with 3 conductive and internal energy generating sources placed on the channel bottom wall. Some geometric and physical parameters were considered as follows: Grashof number from 0 to 10^6, Prandtl number equal to 0.7, Reynolds number from 10 to 1000 and diffusivities from 3 to 100, three source heights (0.075, 0.1, and 0.15) and three channel inclinations (0^0, 45^0 and 90^0). Some results were extensively validated and a mesh independency technique was used. In addition, a time step study was carried out. For Pr =0.7, Re = 100, D = 5 and α = 0º, Nu_B increased for all heights as Gr increased, as it was expected. However, if one fixes Gr to one value up to 3.10^5, Nu_B in body 1 was the highest for H_B = 0.150 and the lowest for H_B = 0.075. This behavior came to be the opposite for Gr ≥ $8x10^5$, and the three bodies presented a more significant difference in Nusselt number. For high Gr, buoyancy forces were predominant and even more predominant for bigger bodies since the energy generation is a volumetric effect. Also, bodies for Hc = 0.15 might have stimulated recirculatoins that could impair heat exchange. For Pr = 0.7, H_B = 0.075, Gr = 10^5, D = 5, and α = 0º, Nu_B on body 1 was higher since it is the first hot body to meet to cold fluid entering the channel. Interestingly, Nu_{B2} and Nu_{B3} were quite the same for this case. It was expected to have lower Nu on downstream bodies in an asset like this, but they were almost equal. In fact, the distance between bodies, Re, and Gr interfered in the thermal wake that led to heating of downstream hot bodies. The effect of the inclination angle study for α = 0º, 45º and 90º, Pr = 0.7, Re = 100, H_B = 0.150 and D = 5 showed that the horizontal channel position presented a lower Nu_B for every Gr and both bodies, 1 and 3. For body 3, this difference was much more significant. There was no significant difference in Nu between 45º and 90^0 for body 3. For Re = 100, 300, 500, 1000, Pr = 0.7, D = 5, α = 0º, H_B = 0.15, τ =20, and for Gr = 10^5 and 10^6, there was no quasi-periodic behavior in time. The least favorable case was for Re = 100 and Gr = 10^6. In this case, there was a strong reversal flow in the upper part of the channel.

6. ACKNOWLEDGEMENTS

The authors thank CNPq for the financial support of two scholarships for the Scientific Initiation Program.

7. REFERENCES

Armaly, B. F., Durst, F., Pereira, J. C. F., Schonung, B., 1983. "Experimental and theoretical investigation of backward-facing step flow". *Journal of Fluid Mechanics*, 127, pp. 473-496.

Aminossadati, S. M. and Ghasemi, B., 2009. "A numerical study of mixed convection in a horizontal channel with a discrete heat source in an open cavity". *European Journal of Mechanics B/Fluids*, 28, pp. 590-598.

Bautista, O., Méndez, F., 2006. "Internal heat generation in a discrete heat source: conjugate heat transfer analysis". *Applied Thermal Engineering*, Vol. 26, 17, pp. 2201-2208.

Bejan, A., 1995. *Convection Heat Transfer*. Wiley, New York, 2nd edition.

Celik, I. B., Ghia, U., Roache, P. J., Freitas, C. J., Coleman, H., Raad, P. E., 2008, "Procedure for estimation and reporting of uncertainty due to discretization in CFD applications". *ASME Journal of Fluids Engineering*, 130, Vol.7, 078001.1-078001.4

Comini, G., Manzam, M., Cortella, G., 1997. "Open boundary conditions for the streamfunction – vorticity formulation of unsteady laminar convection". *Numerical Heat Transfer*, Part B, 31, pp. 217-234.

Figueiredo, J. R., Ganzarolli, M. M., Almeida, P. I. F., 1986. "Convecção natural em cavidades retangulares – solução numérica". *II Congresso Latino-Americano de Transferência de Calor e Matéria*, pp.62-73.

Gartling, D. K., 1980. "A Test problem for outflow boundary conditions – flow over a backward-facing step". *International Journal of Numerical Methods in Fluids*, 11, pp. 953-967.

Guimarães, P. M. and Menon, G. J., 2011. *A mixed convection study in inclined channels with discrete heat sources.* Convection and Conduction Heat Transfer, Intech.

Kim, J. and Moin, P., 1985. "Application of a fractional-step method to incompressible Navier-Stokes equations". *Journal of Computational Physics*, 59, pp. 308-323.

Kuznetsov , G. V. and Maksimov V. I., 2016. "Experimental investigation of the mixed convection of a gas in a rectangular enclosure with a local heat source and heat removal at the outer boundaries". *Journal of Engineering Physics and Thermophysics* Vol. 5, 89, pp. 1241-1246.

Lee, T. and Mateescu, D., 1998. "Experimental and numerical investigation of 2-D backward-facing step flow". *Journal of Fluids and Structures*, 12, pp. 703-716.

Mikhailenko, S. A., Sheremet, M. A., Mohamed, A. A., 2018. "Convective-radiative heat transfer in a rotating square cavity with a local heat-generating source". *International Journal of Mechanical Sciences*, pp. 530-540.

Muthtamilselvan, M., Prakash, D., Doh, D.H., 2014. "Effect of non-uniform heat generation on unsteady MHD flow over a vertical stretching surface with variable thermal conductivity". *Journal of Mechanics*, Vol. 2, 30, pp. 199-208.

Pinto, R. J., 2016. *Estudo numérico do problema conjugado de convecção nista em duto contendo fontes condutoras e geradoras de energia interna.* Ph.D. thesis, Universidade Federal de Itajubá, Itajubá, Brasil.

Rahman, M. M., Alim, M. A., Saha, S., 2009. "Mixed convection in a square cavity with a heat-conducting horizontal square cylinder". *Suranaree Journal of Science and Technology*, Vol. 2, 17, pp. 139-153.

Wong, H. H., Raithby, G. D., 1979. "Improved finite – difference methods based on a critical evaluation of the approximation errors". *Numerical Heat Transfer*, 2, pp. 139-163.

Xu , S., Wang , W., Guo , Z., Hu, X., Guo , W., 2016. "A multi-channel cooling system for multiple heat source". *Thermal Science*, Vol. 6, 20, pp. 1991-2000.

8. RESPONSIBLE NOTICE

The authors are the only responsible for the printed material included in this paper.